Supplementary Materials for the manuscript:

Microbial community dynamics and coexistence in a sulfide-driven phototrophic bloom

Authors

Srijak Bhatnagar*, Elise S. Cowley*, Sebastian H. Kopf, Sherlynette Pérez Castro, Sean Kearney, Scott C. Dawson, Kurt Hanselmann, S. Emil Ruff

Supplementary Materials and Methods

16S rRNA gene libraries and construction of phylogeny

From the DNA of Sample 7A3 (Replicate hole A, at 25 cm depth at time point 7) clone library was made in following way. The 16S rRNA gene was amplified using 27F (Bacterial - AGAGTTTGATCMTGGCTCAG) or 4Fa (Archaeal - TCCGGTTGATCCTGCCRG) forward primer and 1391R (broad range - GACGGGCGGTGTGTRCA) reverse primer. The PCR product was cleaned using Promega Wizard® PCR Cleanup system and cloned using pGEM®-T easy system using manufacturer supplied standard protocol (Promega Corporation, Madison, WI). Briefly, the cleaned PCR product was ligated in vector, followed by vector cloning into Promega JM109 competant cells. The transformed cells were selected and screened using blue-white colony screening on LB plate with ampicillin, X-gal, and IPTG. The transformed cells were grown in liquid LB broth with ampicillin for 12 hours and the plasmid was extracted using Promega PureYieldTM plasmid system. The plasmid was send to Sequetech DNA Sequencing Service (Mountain View, CA) for Sanger sequencing from one end using the T7 primer.

16S rRNA gene phylogeny was calculated using ARB/SILVA (Ludwig et al., 2004) and the SILVA database SSU Ref NR 132 (Quast et al., 2013). We added the sequences to the SILVA tree using the ARB maximum parsimony quick-add tool and chose near full-length (>1300 nucleotides) reference sequences from neighboring clades and isolates. We aligned these sequences using SINA (Pruesse et al., 2012) and manually curated the alignment based on ribosomal secondary structure. This alignment was used to calculate a tree with the RAxML8 algorithm (Stamatakis, 2014) and a positional variability filter including only conserved positions in the alignment with ≤3.1% mutation rate. The final alignment had 1007 valid columns encompassing the *E. coli* reference positions 1785-40339. The tree was calculated with 100 iterations of which the most robust tree was selected. The partial gene sequences from this study were added to the consensus tree using the same positional variability filter without changing the overall tree topology.

Supplementary Results

Physicochemistry

Within the first three days the pH decreased between 1-2 units in all layers, from around pH 9 to pH 7 at 5 cm water depth (7.7±1.0), from pH 8 to pH 7 at 10 cm (7.3±0.7) and from pH 8 to pH 6.3 at 25 (6.7±0.8) and 35 cm (6.8±0.7) (Figure 2). Over the 15-day sampling period, the pH at 5 cm (7.3±0.8) and 10 cm (6.9±0.6) water depth showed more variation than at 25 cm (6.5±0.6) and 35 cm (6.5±0.5). At depths within and below the bloom, pH was very constant between 6 and 6.3.

The Fe(II) concentration at 5 cm and 10 cm was < 5 μM (Figure S4). The Fe(II) concentration at these depths showed less fluctuation over the 15 days of sampling as compared to 25 cm and 35 cm. With an average range of 10 – 12 μM concentration, samples from 25 cm had the highest concentration of Fe(II). When compared to Fe(II), the Fe(III) concentrations were consistently lower at all depths between 1-5 μM. With roughly 20-25 μM of total iron, 25 cm samples had the highest iron concentration (Figure S5).

Nitrate concentration showed more fluctuation over the sampling period at shallower depths, specifically at 5 cm and 10 cm, with a short-lived nitrate spike 5 days after the start of the experiment (Figure S5). This spike coincides with a concentration dip in the major ions suggesting an input of nitrate rich freshwater, potentially from fertilizer-rich soil runoff. The nitrate concentrations at 25 cm were slightly higher than at other depths in the water column.

Ammonium and acetate concentrations were highest at 35 cm depth (up to 4 mM and 1.5 mM, respectively) with significantly lower concentrations at the shallower sampling points (25 cm, 10 cm, 5 cm) including no detectable ammonium throughout the entire experiment at the surface (5 cm). This indicates a source of ammonium and acetate at depth which is consistent with ammonification and acetate generation from fermentative organic matter degradation of the decaying seagrass underneath.

In addition, measurements of sodium, fluoride, chloride, bromide, phosphate, lithium, magnesium, lactate, formate, succinate, propionate, butyrate and glucose were made on all samples collected. The values are not shown for reasons of clarity, but the raw data are still available. The values for sodium and chloride were outside the range of the standard calibration curve, hence these values were not analyzed.

Supplementary Figures

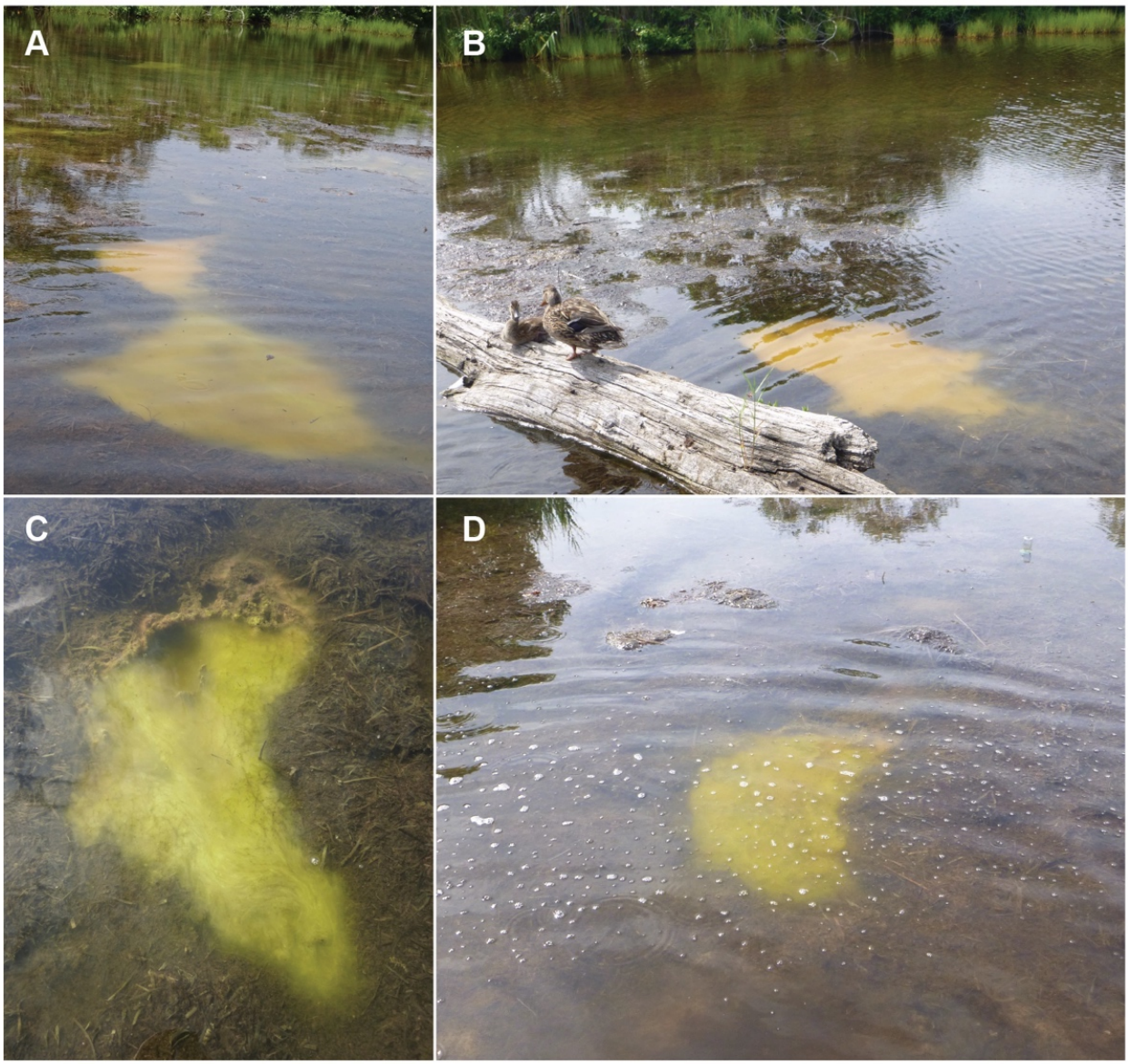

Figure S1: Pictures of natural blooms in Trunk River. **B** is the natural bloom shown in the aerial overview Figure 1A. **C** is a close-up of bloom **D**.

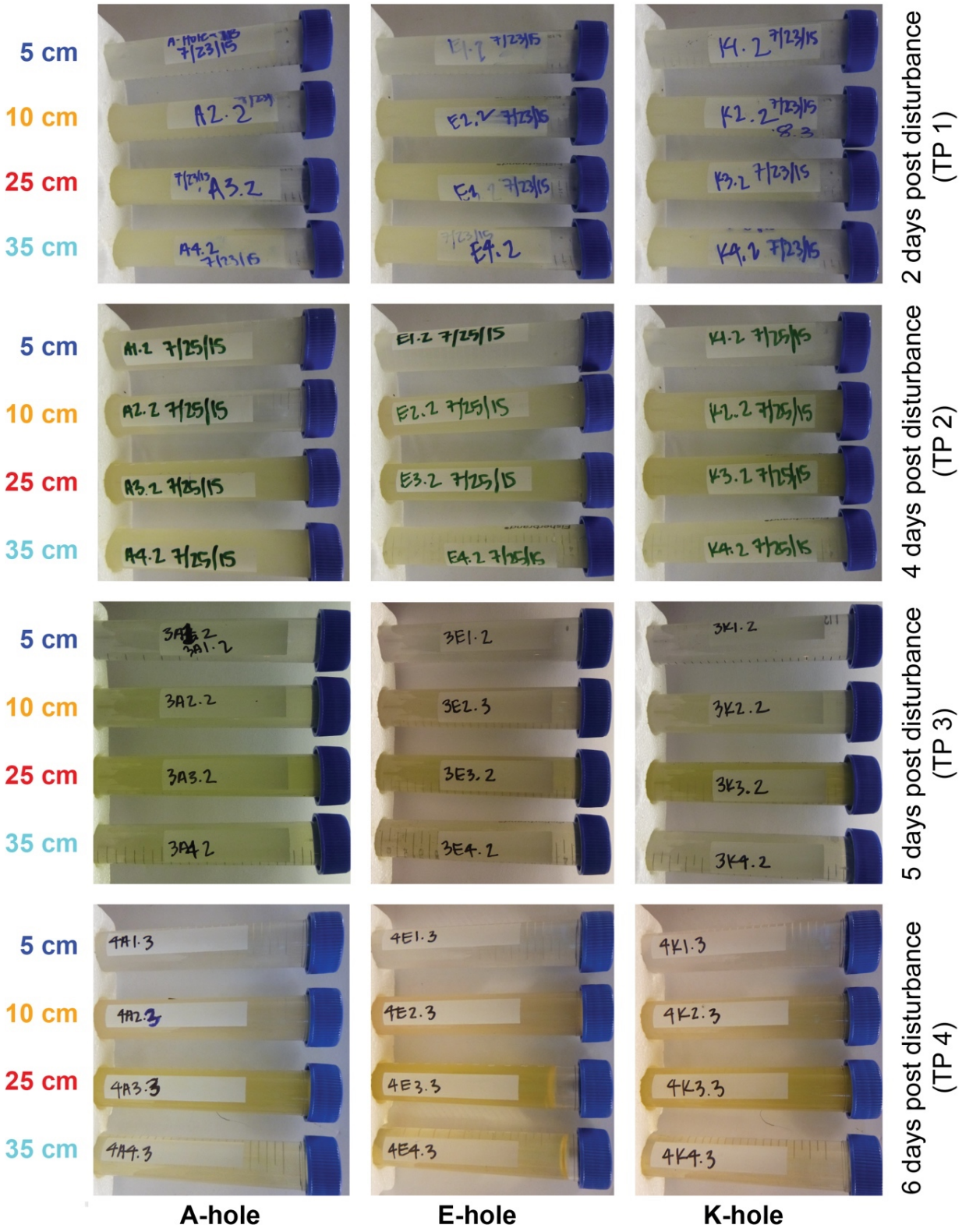
5 cm
10 cm
25 cm
35 cm
2 days post disturbance (TP 1)
4 days post disturbance (TP 2)
5 days post disturbance (TP 3)
6 days post disturbance (TP 4)
A-hole
E-hole
K-hole

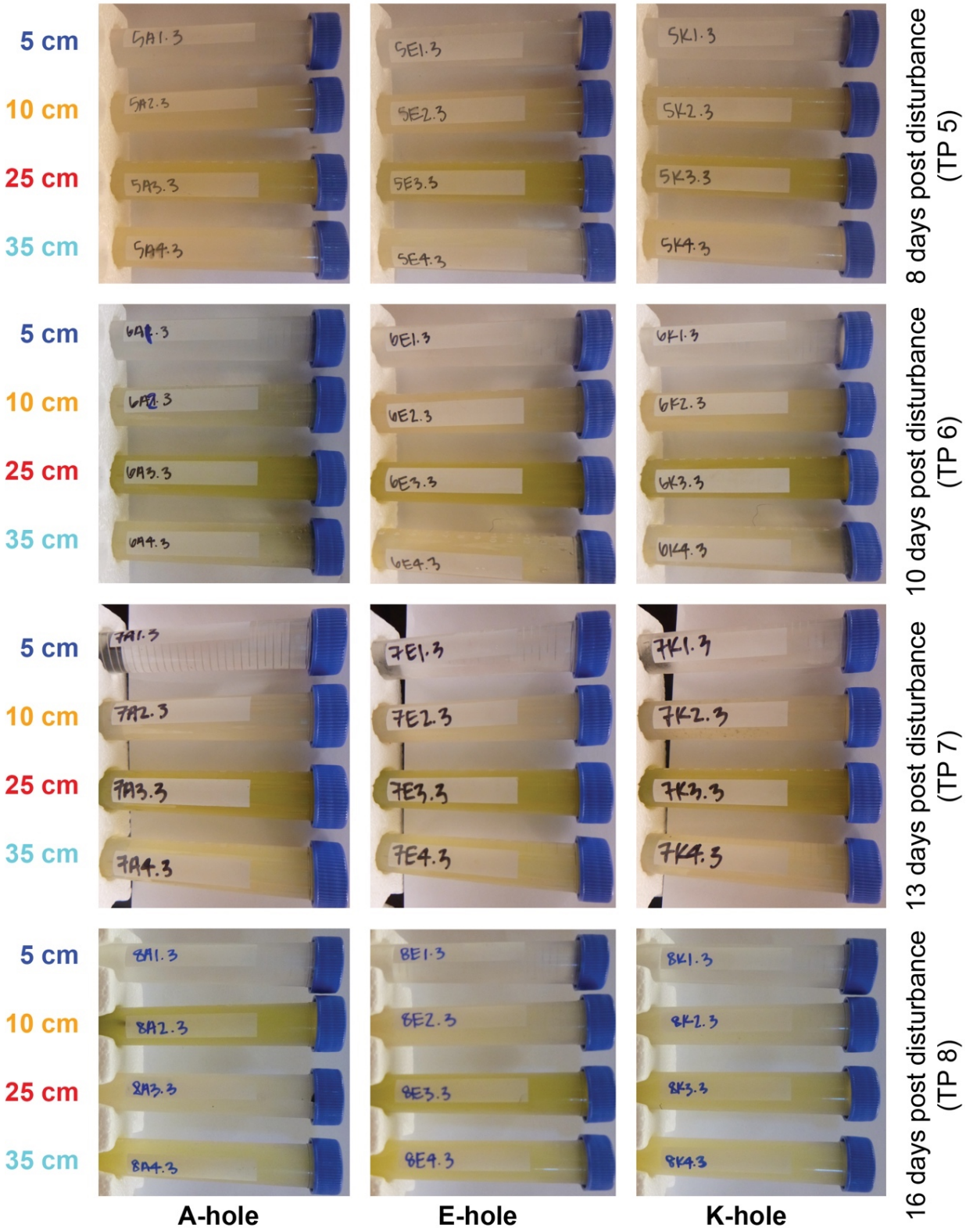

Figure S2: Color and appearance of samples from all holes, depths, and timepoints.

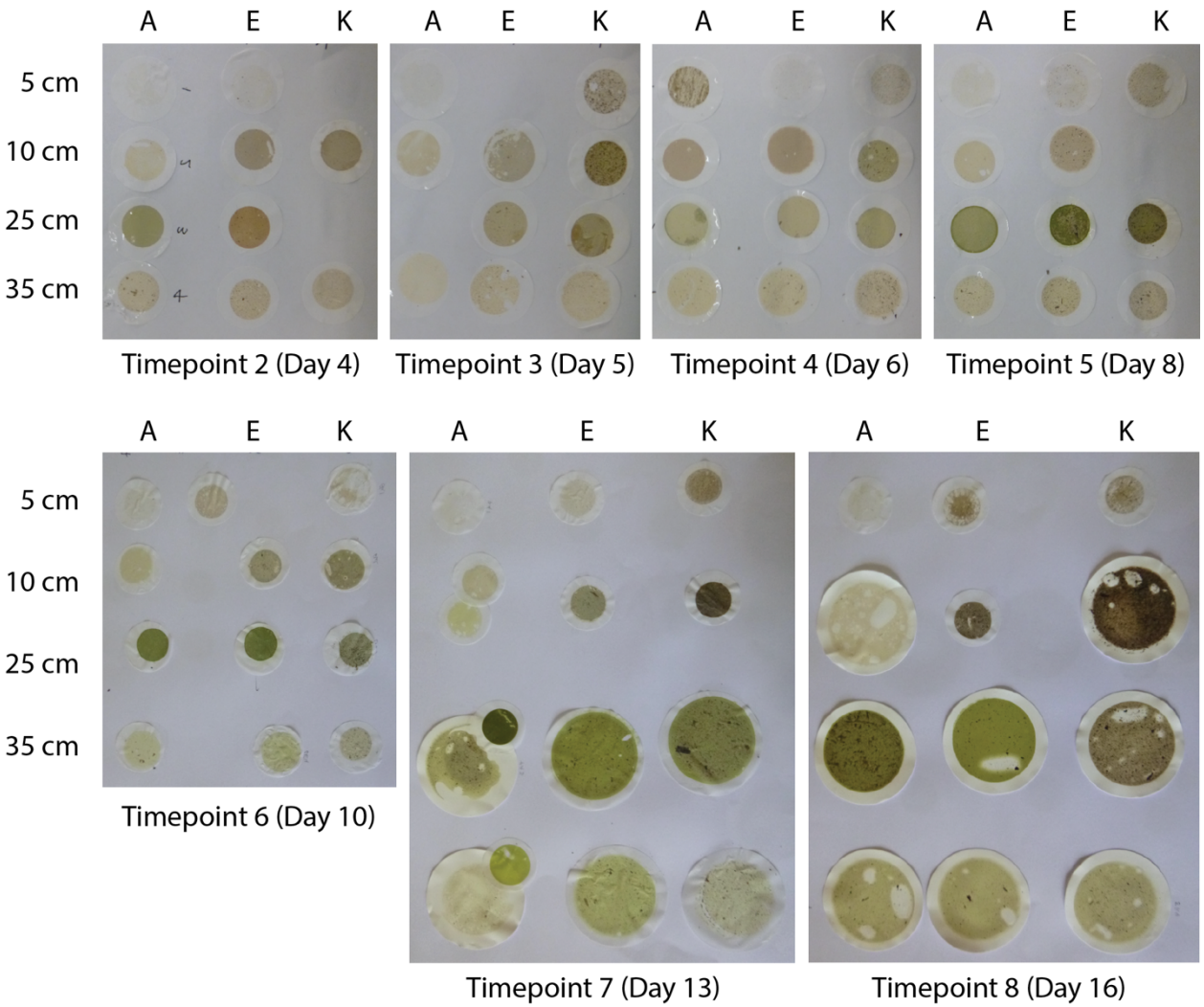

Figure S3: Filters that were used for biomass measurements and spectral analysis.

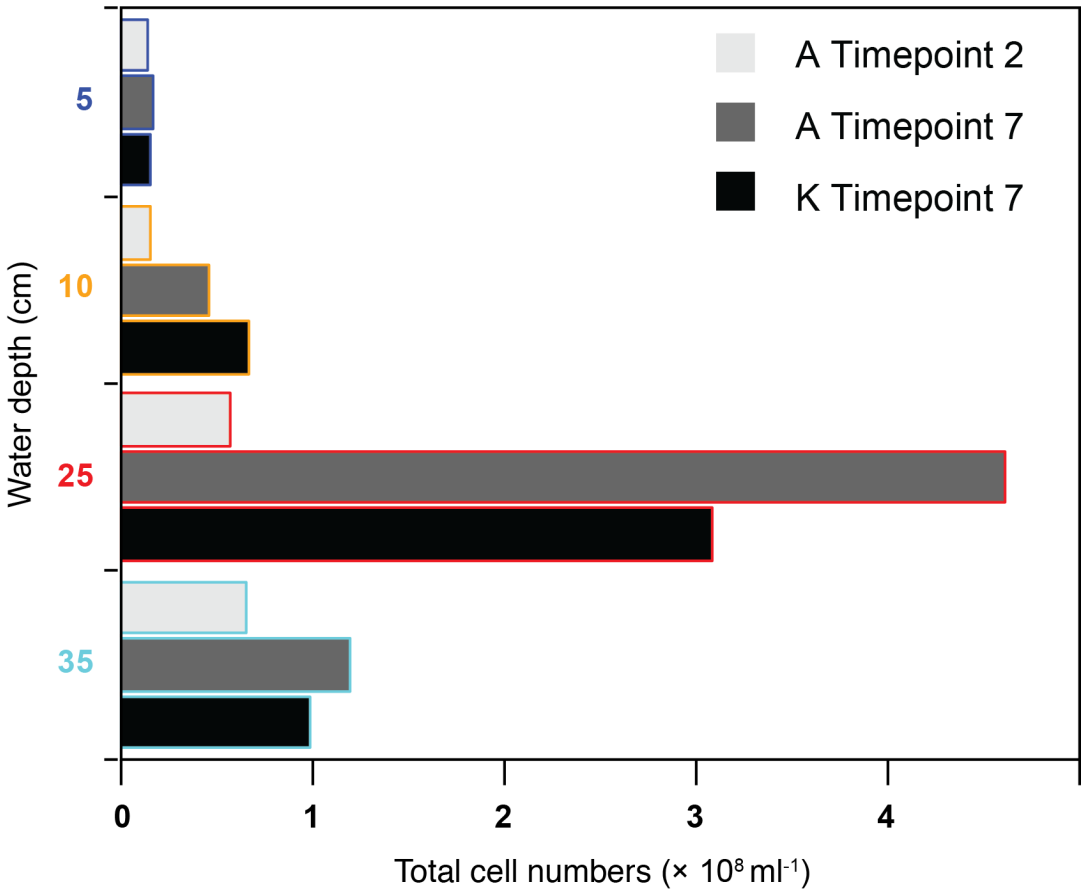

Figure S4: Total cell count of three samples (A2, A7 and K7) showing the differences in cell numbers between layers at the beginning and close to end of the experiment, corroborating the results obtained from biomass measurements.

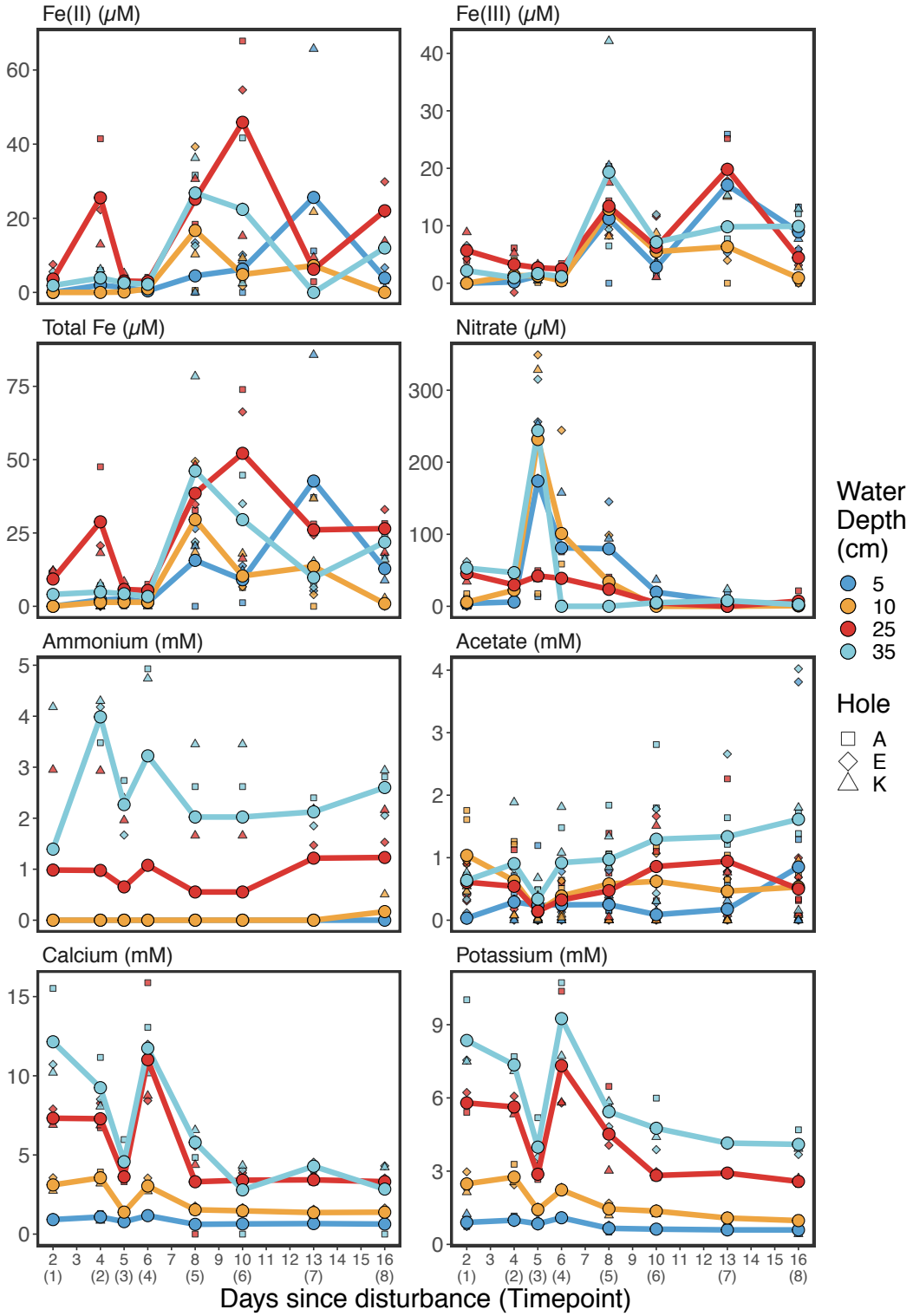

Figure S5: **Physicochemistry**. Iron, nitrate, ammonium, acetate, Ca^{2+}, and K^{+} measurements. The x-axis shows days since disturbance, y-axis the respective units.

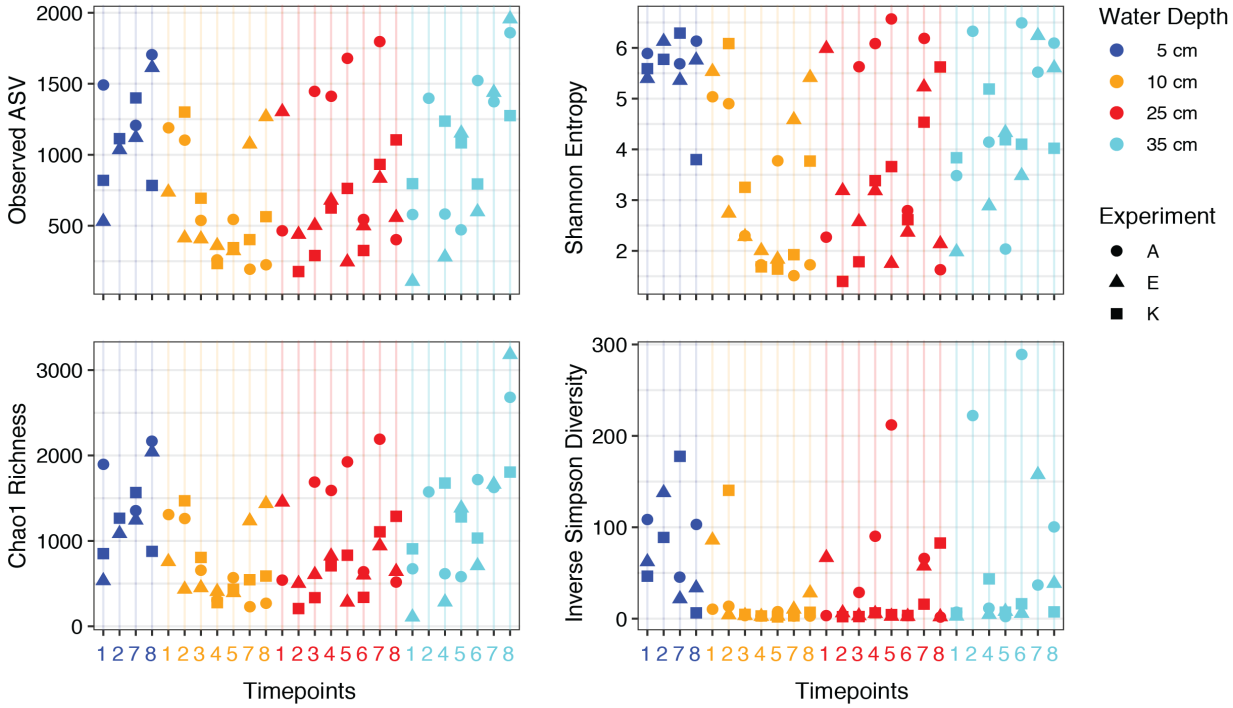

Figure S6: Individual diversity Indices of all samples showing the decrease in diversity in the bloom, especially in layer 2 and 3.

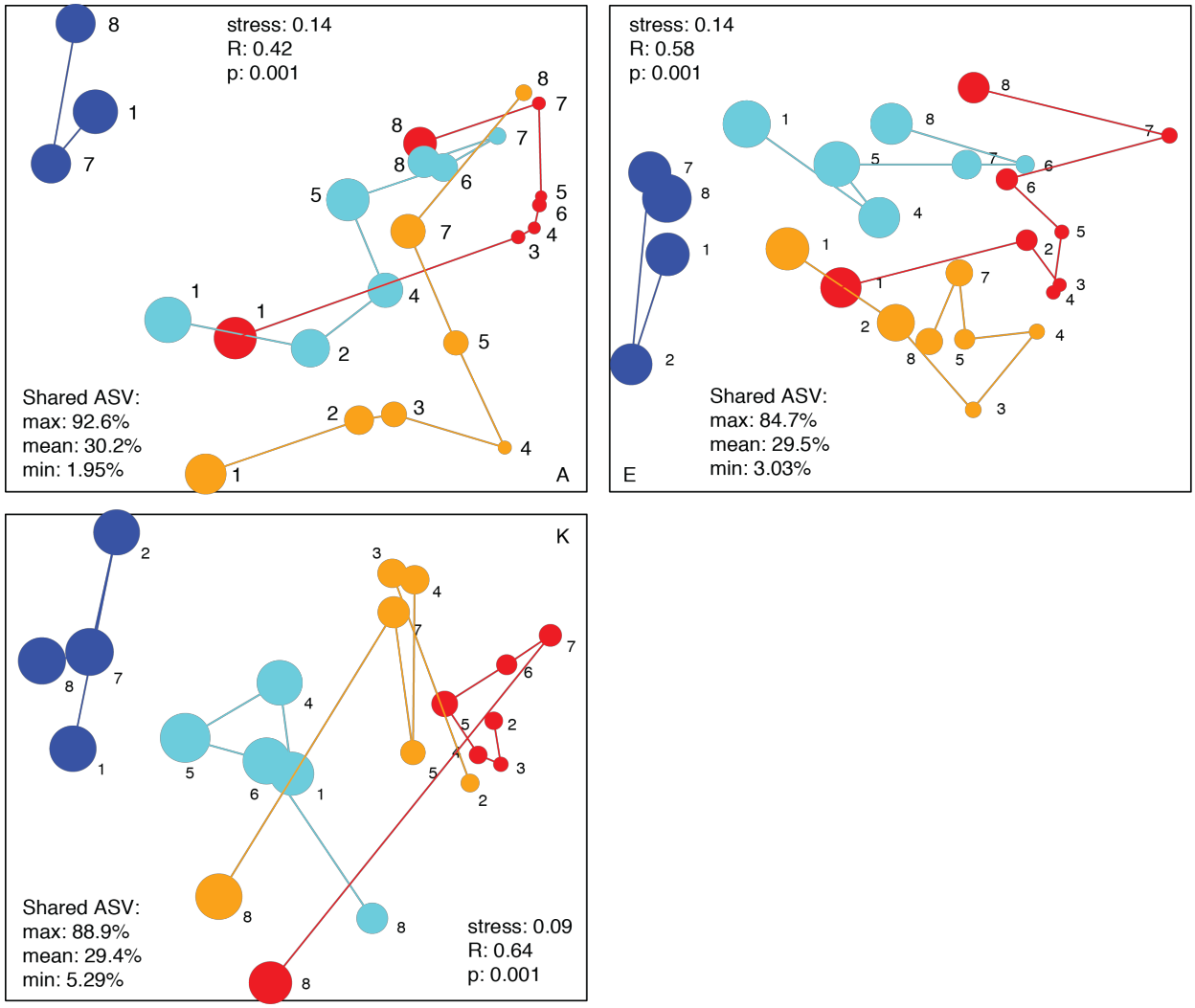

Figure S7: Trajectories of community structure in hole A, E and K. Circle size represents average Shannon Diversity across three replicate holes. Sampling time points are indicated as numbers. ASV: Amplicon Sequence Variant. Shared ASV show maximal, minimal and average percentage of shared ASV between any pair of two samples. Analysis of similarity (ANOSIM) was used to test whether the communities of each depth layer were similar. R and p values show that the groups were overlapping, but significantly different.

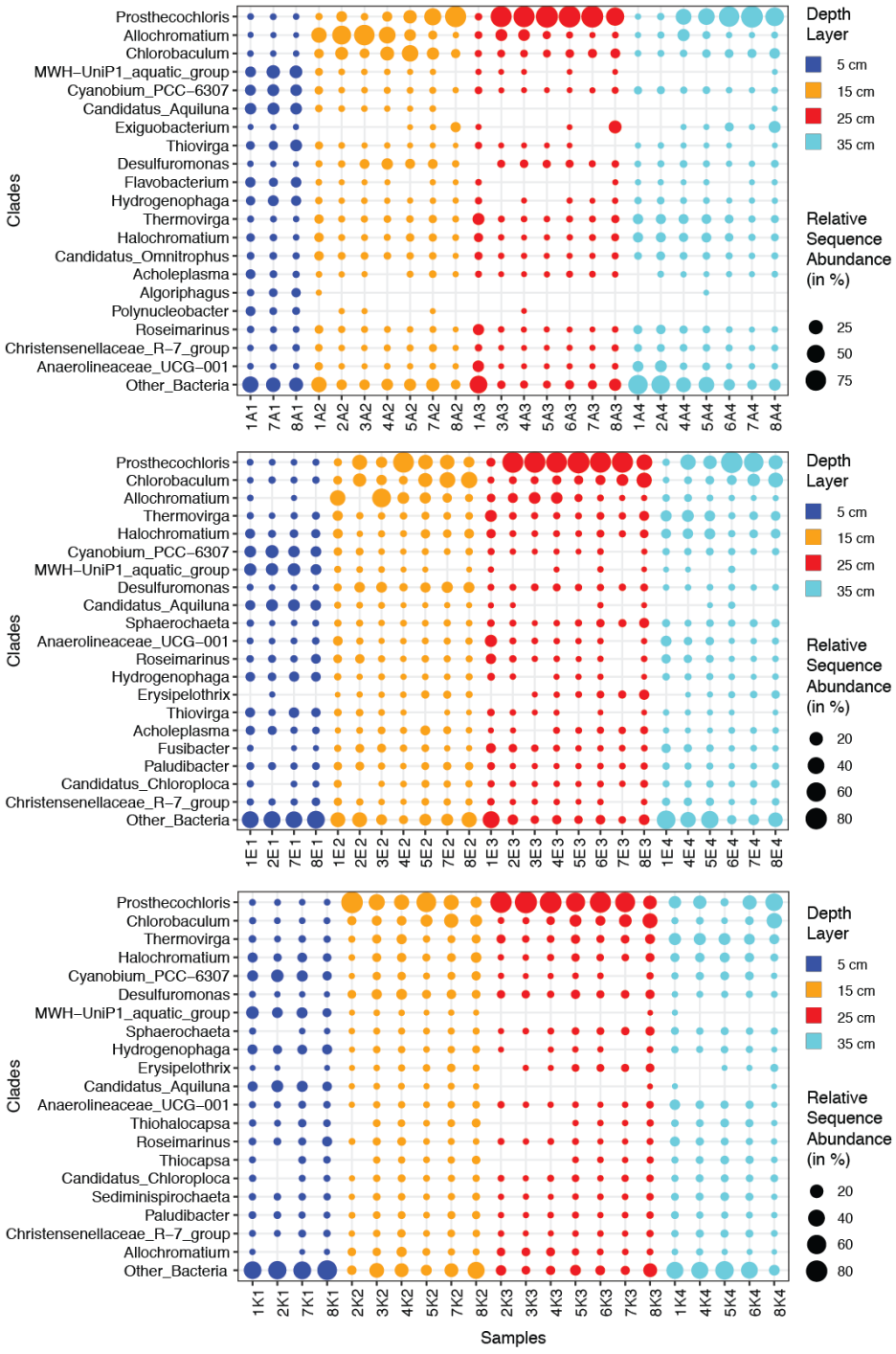

Figure S8A: Relative sequence abundance of the 20 most prominent genera in all three replicate experiments. Sample names include time point, experiment and depth, e.g. 3E2: Timepoint 3, E-hole, depth 3 (25 cm). A samples in top panel, E in middle panel, K in bottom panel).

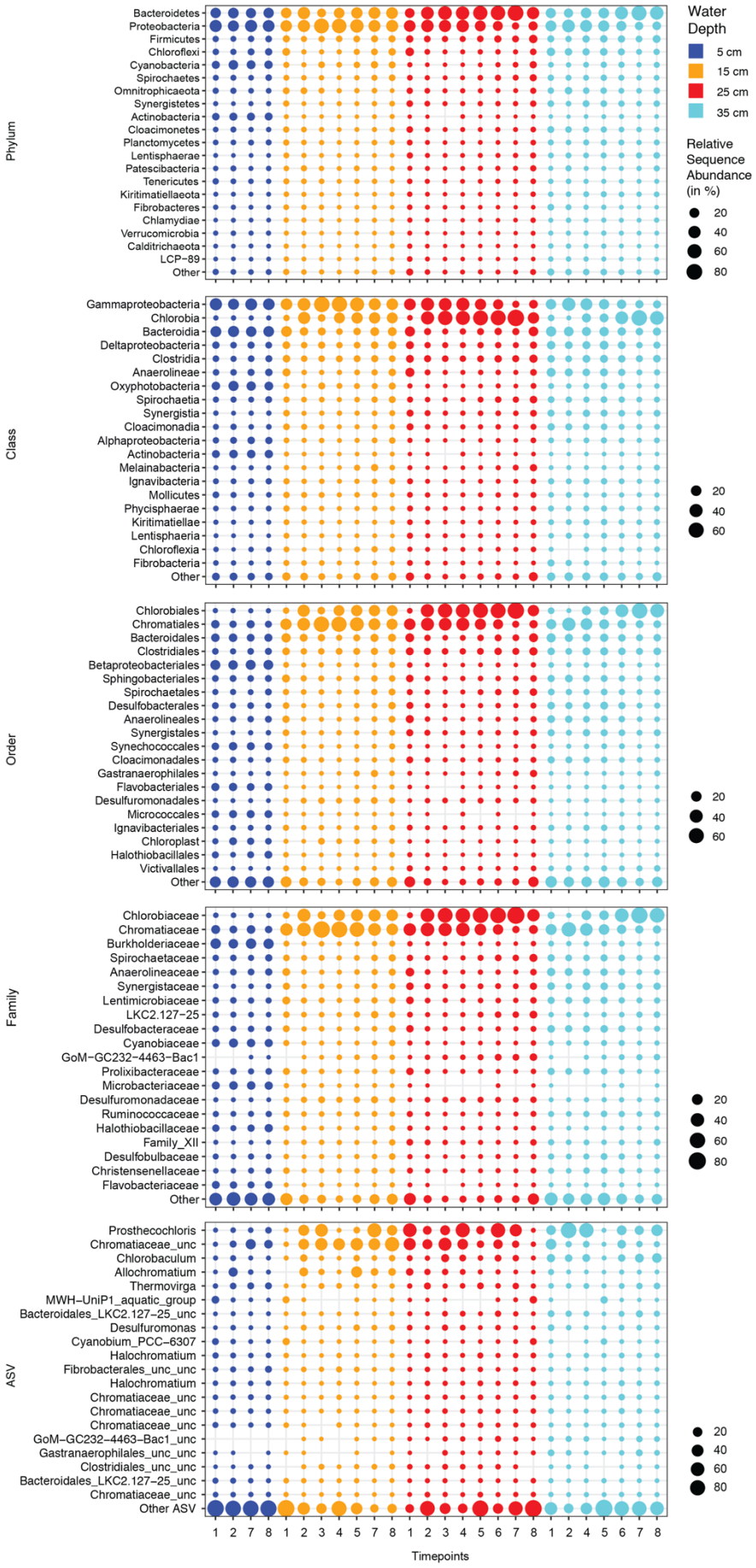
Phylum
Bacteroidetes
Proteobacteria
Firmicutes
Chloroflexi
Cyanobacteria
Spirochaetes
Omnitrophicaeota
Synergistetes
Actinobacteria
Cloacimonetes
Planctomycetes
Lentisphaerae
Patescibacteria
Tenericutes
Kiritimatiellaeota
Fibrobacteres
Chlamydiae
Verrucomicrobia
Calditrichaeota
LCP-89
Other
Class
Gammaproteobacteria
Chlorobia
Bacteroidia
Deltaproteobacteria
Clostridia
Anaerolineae
Oxyphotobacteria
Spirochaetia
Synergistia
Cloacimonadia
Alphaproteobacteria
Actinobacteria
Melainabacteria
Ignavibacteria
Mollicutes
Phycisphaerae
Kiritimatiellae
Lentisphaeria
Chloroflexia
Fibrobacteria
Other
Order
Chlorobiales
Chromatiales
Bacteroidales
Clostridiales
Betaproteobacteriales
Sphingobacteriales
Spirochaetales
Desulfobacterales
Anaerolineales
Synergistales
Synechococcales
Cloacimonadales
Gastranaerophilales
Flavobacteriales
Desulfuromonadales
Micrococcales
Ignavibacteriales
Chloroplast
Halothiobacillales
Victivallales
Other
Family
Chlorobiaceae
Chromatiaceae
Burkholderiaceae
Spirochaetaceae
Anaerolineaceae
Synergistaceae
Lentimicrobiaceae
LKC2.127-25
Desulfobacteraceae
Cyanobiaceae
GoM-GC232-4463-Bac1
Prolixibacteraceae
Microbacteriaceae
Desulfuromonadaceae
Ruminococcaceae
Halothiobacillaceae
Family_XII
Desulfobulbaceae
Christensenellaceae
Flavobacteriaceae
Other
ASV
Prosthecochloris
Chromatiaceae_unc
Chlorobaculum
Allochromatium
Thermovirga
MWH-UniP1_aquatic_group
Bacteroidales_LKC2.127-25_unc
Desulfuromonas
Cyanobium_PCC-6307
Halochromatium
Fibrobacterales_unc_unc
Halochromatium
Chromatiaceae_unc
Chromatiaceae_unc
Chromatiaceae_unc
GoM-GC232-4463-Bac1_unc
Gastranaerophilales_unc_unc
Clostridiales_unc_unc
Bacteroidales_LKC2.127-25_unc
Chromatiaceae_unc
Other ASV
1 2 7 8 1 2 3 4 5 7 8 1 2 3 4 5 6 7 8 1 2 4 5 6 7 8
Timepoints
Water Depth
5 cm
15 cm
25 cm
35 cm
Relative Sequence Abundance (in %)
20
40
60
80

Figure S8B: Relative sequence abundance of the 20 most prominent clades on phylum, class, order and family level, as well as the 20 most sequence abundant ASVs (amplicon sequence variants). The suffix _unc and _unc_unc refers to ASV of an unclassified genus or family, respectively. These ASV belong to uncultured lineages and - due to their high relative abundance - are very likely not sequence errors. Values represent average across three replicate experiments. Note: Based on the new SILVA taxonomy, the Chlorobi are now a subphylum of the Bacteroidetes.

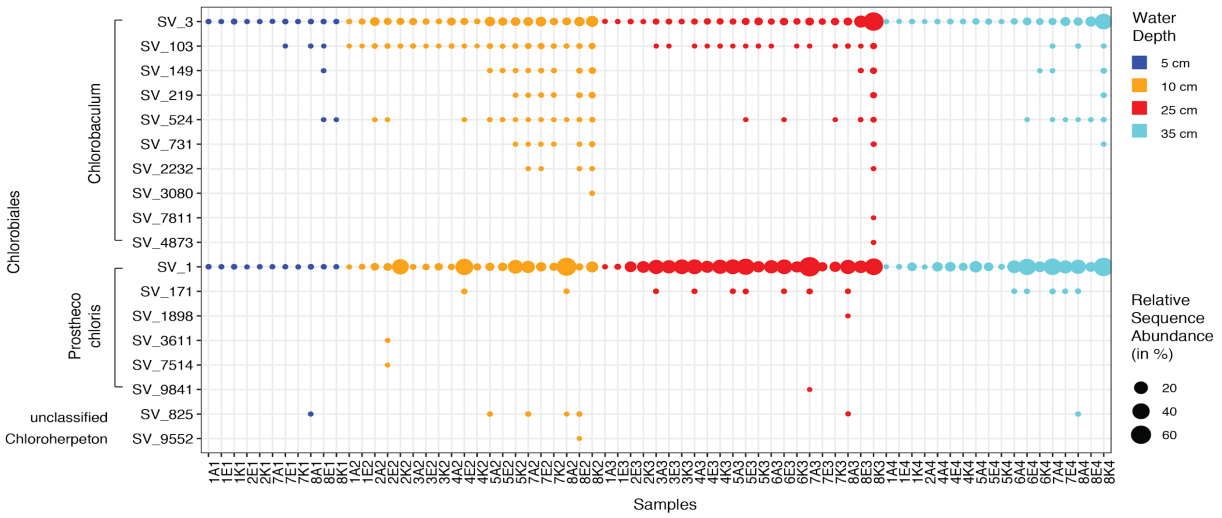

Figure S9: Relative sequence abundance of ASV within the *Chlorobiales* order. Sample names include time point, experiment and depth, e.g. 3E2: Timepoint 3, E-hole, depth 3 (25 cm). All samples, and replicate experiments are shown.

	5 cm	10 cm	25 cm	35 cm
Prosthecochloris	1	2.23	2.61	2.07
Chlorobaculum	1	2.37	2.24	2.45
Allochromatium	1	5.76	3.73	1.95
Thermovirga	1	1.05	2.05	1.64
Halochromatium	1	1.64	1.95	1.47
Cyanobium_PCC-6307	1	1.03	0.83	1.04
MWH-UniP1_aquatic_group	1	1.15	0.95	0.99
Desulfuromonas	1	3.77	5.27	3.09
Candidatus_Aquiluna	1	0.76	0.56	0.86
Hydrogenophaga	1	1.49	1.11	1.06
Sphaerochaeta	1	1.21	1.57	1.83
Thiovirga	1	0.73	0.87	0.57
Exiguobacterium	1	3.74	6.61	1.19
Anaerolineaceae_UCG-001	1	0.84	1.47	1.33
Flavobacterium	1	0.67	0.49	0.65
Roseimarinus	1	1.54	2.37	2.00
Erysipelothrix	1	1.25	1.54	2.32
Candidatus_Chloroploca	1	1.80	2.45	1.67
Christensenellaceae_R-7_group	1	1.46	2.15	1.37
Paludibacter	1	1.51	1.79	1.74
Other	1	1.42	1.59	1.30

Figure S10: Relative change of sequence abundance of ASVs between surface (V1) and deeper layers (V2-4)

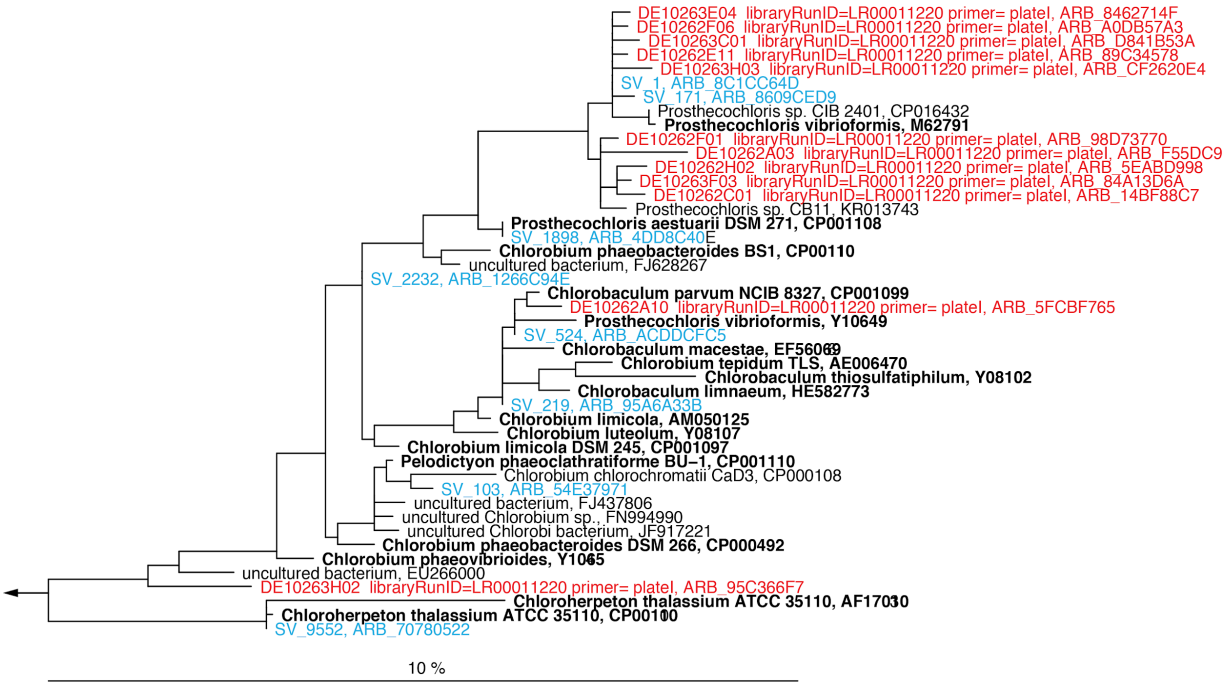

Figure S11: A phylogenetic tree depicting the affiliation of ASVs (blue), gene library sequences (red) and neighboring reference sequences (cultured isolates are in bold face). The Genbank accession of reference sequences is provided in the node labels. Scale bar shows estimated sequence divergence. Note: Accession numbers will be provided once the recently submitted sequences are processed and public.

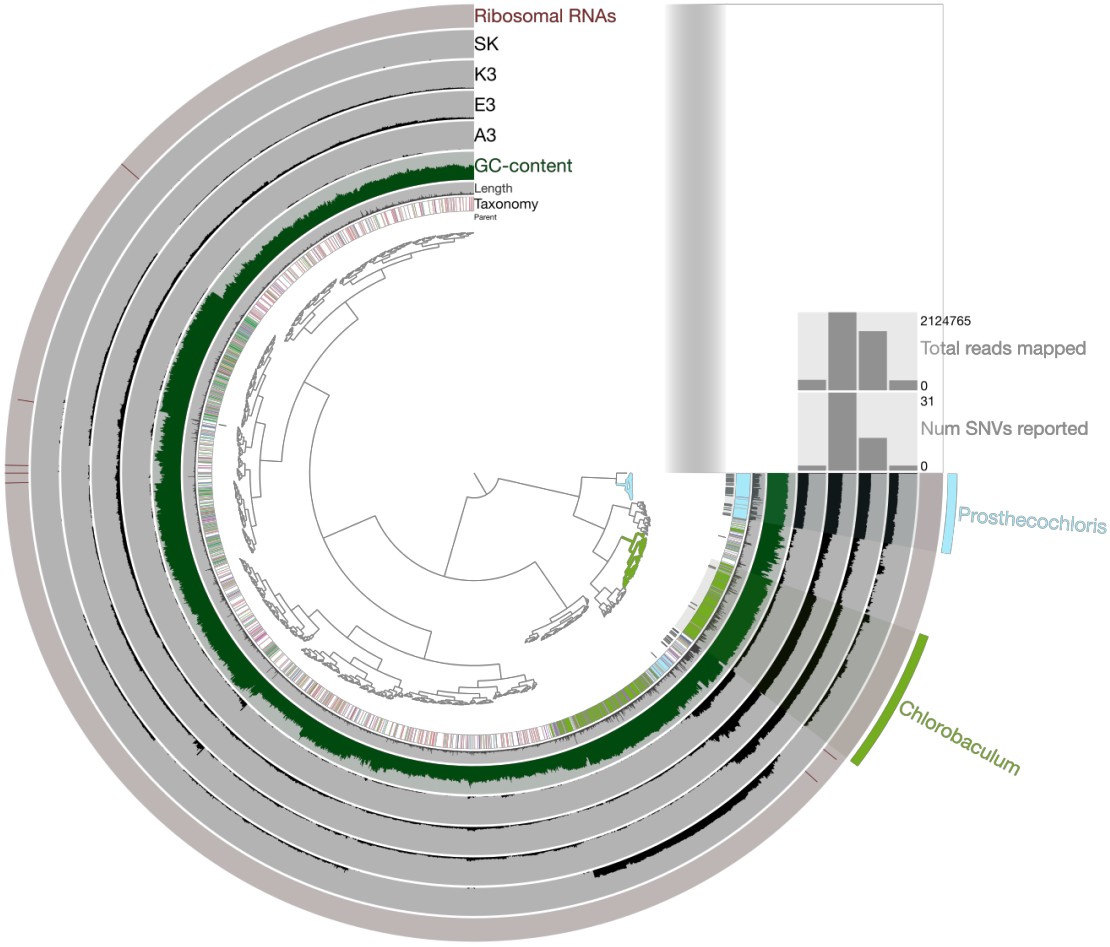

Figure S12: Circular map of metagenome-assembled genomes (MAGs) visualized using Anvi'o. The clustering dendrogram for contigs is based upon taxonomy, contig length, GC-content, and ribosomal RNA operons (from inner to outer rings) [2]. Bin 10 (*Prosthecochloris sp.)* and Bin 6 (*Chlorobaculum sp.)* metagenome-assembled genomes are highlighted.

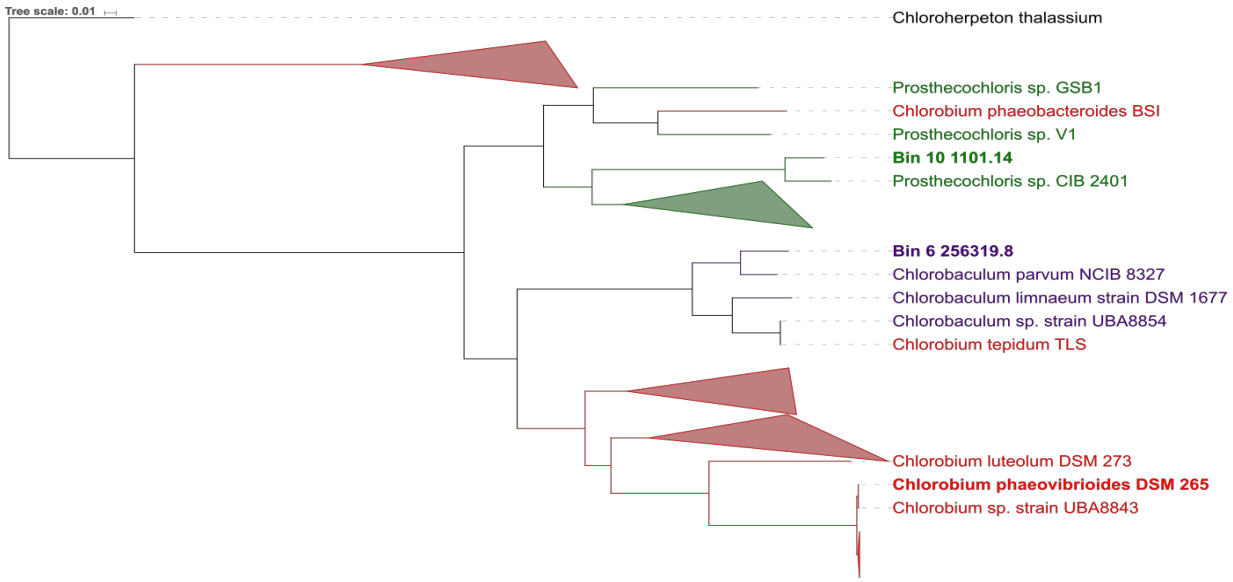

Figure S13: Hierarchical clustering analysis showing *Chlorobaculum parvum* NCBI 8327 as the closest genome to Bin 6 (ANI value 85.13%). *Prosthecochloris sp.* CIB 2401 is the closest genome to Bin 10. The scale bar represents the average number of substitutions per site.

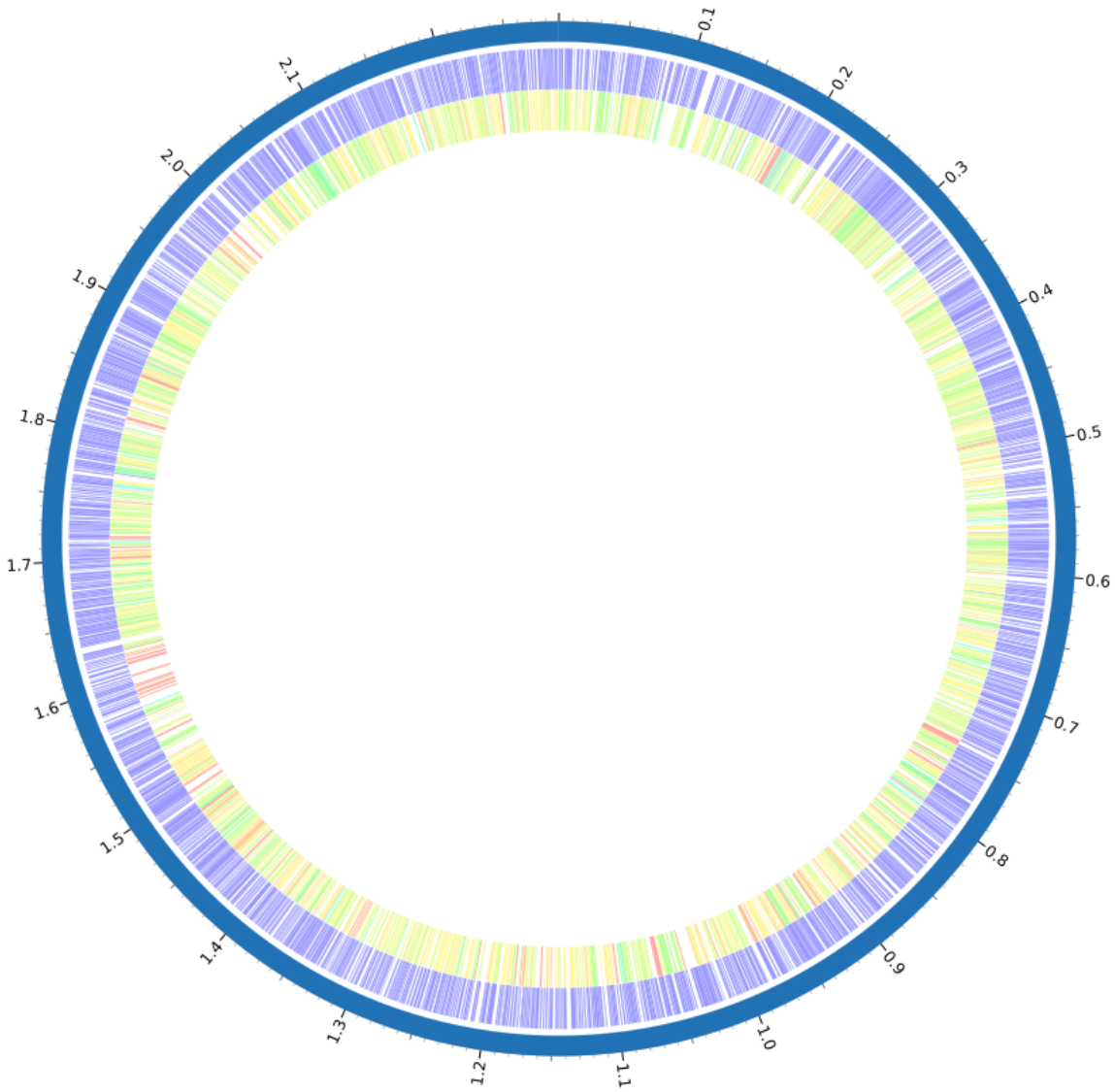

187

Percent protein sequence identity

Bidirectional best hit	100	99.9	99.8	99.5	99	98	95	90	80	70	60	50	40	30	20	10
Unidirectional best hit	100	99.9	99.8	99.5	99	98	95	90	80	70	60	50	40	30	20	10

188

189 **Figure S14:** Protein comparison of the reconstructed population genome (Bin 6)
190 compared against the genome closest neighbor *Chlorobaculum parvum* NCBI 8327.
191 Rings from outside to inside: the contig of the reference species, the reference bacterial
192 species and the potentially novel population genome with the color scale representing
193 the protein similarity.

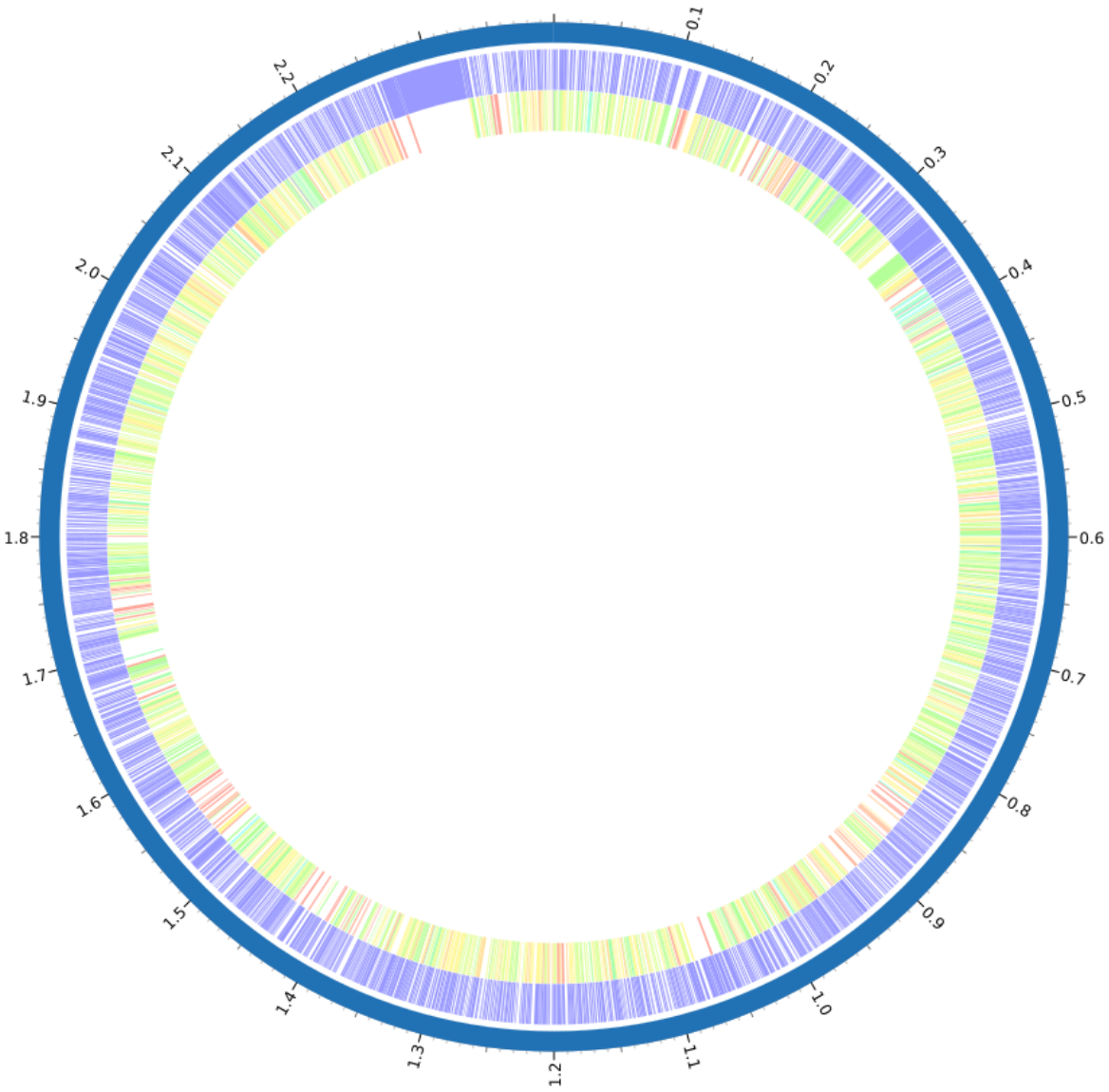

194

Percent protein sequence identity

Bidirectional best hit	100	99.9	99.8	99.5	99	98	95	90	80	70	60	50	40	30	20	10
Unidirectional best hit	100	99.9	99.8	99.5	99	98	95	90	80	70	60	50	40	30	20	10

195

196 **Figure S15:** Protein comparison of the reconstructed population genome (Bin 10)
197 compared against the genome closest neighbor *Prosthecochloris sp.* CIB 2401. Rings
198 from outside to inside: the contig of the reference species, the reference bacterial
199 species and the potentially novel population genome with the color scale representing
200 the protein similarity.
201

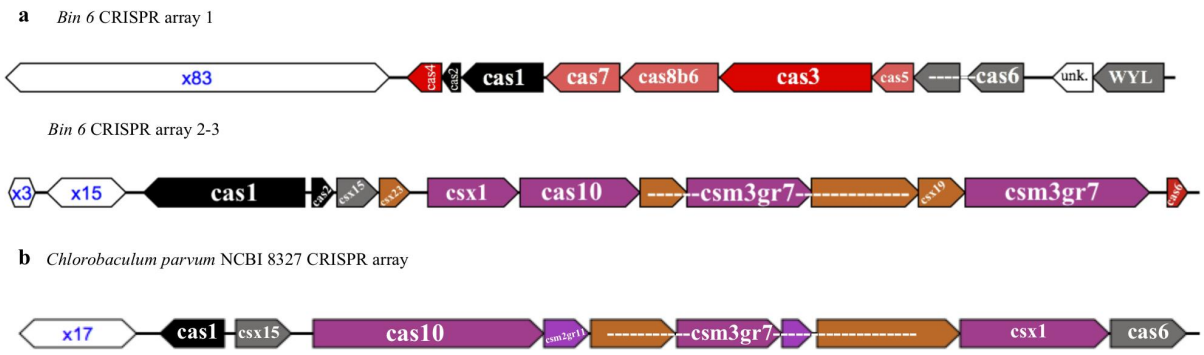

Figure S16: CRISPR arrays and *cas* genes predictions from (a) Bin 6 and (b) *Chlorobaculum parvum* NCBI 8327. CRISPR arrays are in white with the number of repeats, and *cas* genes are color-coded according to types/subtypes. Cas1 and cas2, which are present in most known CRISPR-Cas systems, are in black; cas3 and cas10, which are the signatures of CRISPR-Cas systems types along with Cas9 (Type II), are in red (Type I) and purple (Type III), respectively; variants of the multi-subunit complex (csm), cas10, and *csx* Type III genes are also in purple, and dispensable components, such as cas6, are in gray [7].

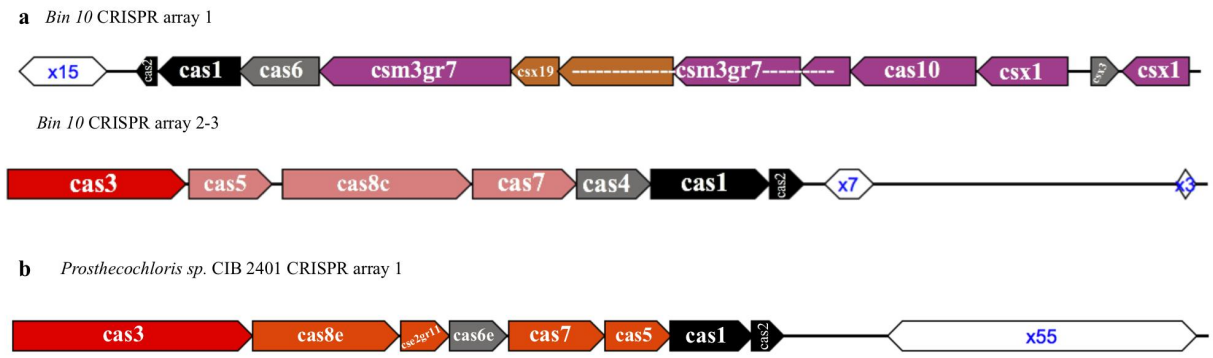

212
213 **Figure S17**. CRISPR arrays and *cas* genes predictions from (a) Bin 10 and (b)
214 *Prosthecochloris sp.* CIB 2401. CRISPR arrays are in white with the number of repeats,
215 and *cas* genes are color-coded according to types/subtypes. Cas1 and cas2, which are
216 present in most known CRISPR-Cas systems, are in black; cas3 and cas10, which are
217 the signatures of CRISPR-Cas systems types along with Cas9 (Type II), are in red
218 (Type I) and purple (Type III), respectively; variants of the multi-subunit complex (csm),
219 cas10, and *csx* Type III genes are also in purple, and dispensable components, such as
220 cas6, are in gray [7].
221

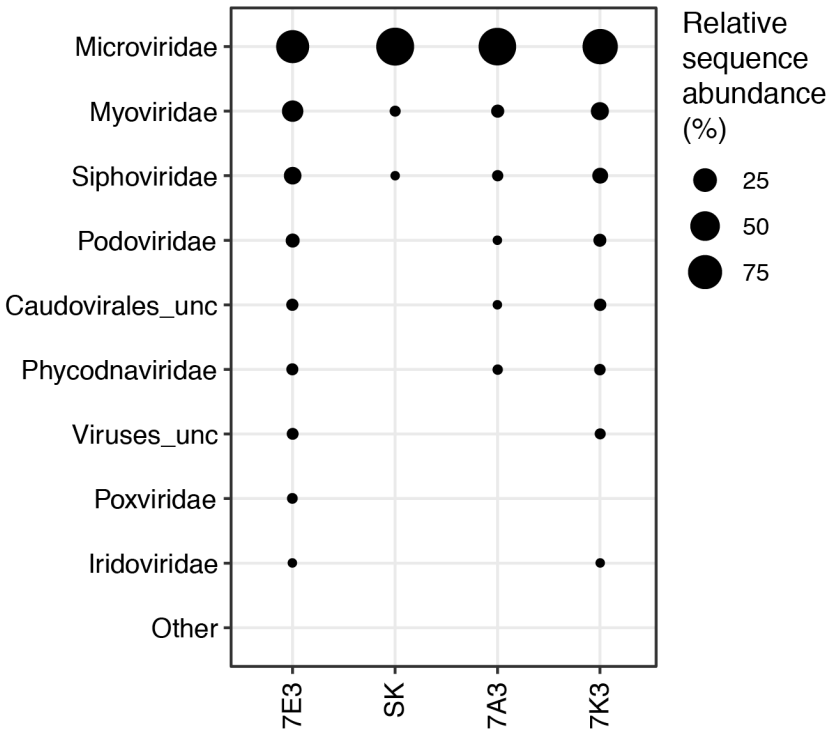

Figure S18. Relative sequence abundance of viral family-level clades based on viral sequences retrieved from metagenomes of timepoint 7 (7A3, 7E3 and 7K3) and from a phototrophic enrichment culture (SK). Unclassified family-level clades are marked by the suffix _unc.

231 Table S1: Overview of sequencing output and diversity indices

	M.reads	M.sobs.r.mean	M.chao1.r.mean	M.invs.r.mean	M.SSOabs.nr	M.SSOrel.nr	M.shan.r.mean	M.SSOabs.pc	M.SSOrel.pc
1A1	115879	1489	1893	108	9	28	5.9	0.4	1.3
1A2	13215	529	533	62	0	6	5.4	0	1.1
1A3	32266	821	853	47	1	6	5.6	0.1	0.7
1A4	30906	1033	1080	138	0	15	6.1	0	1.4
1E1	57122	1116	1244	88	1	16	5.8	0.1	1.2
1E2	63196	1205	1361	46	2	13	5.7	0.1	0.9
1E3	65596	1124	1247	22	2	12	5.4	0.2	0.9
1E4	65227	1410	1564	179	7	37	6.3	0.4	2.3
1K1	138540	1687	2176	103	6	28	6.1	0.2	1.2
1K4	125417	1623	2022	34	3	25	5.8	0.1	1.1
2A2	49647	784	861	6	0	13	3.8	0	1.5
2A4	41419	1180	1321	10	3	13	5	0.2	1
2E1	19251	738	754	86	0	5	5.5	0	0.7
2E2	53217	1109	1261	13	3	25	4.9	0.2	1.9
2E3	29494	412	437	4	0	1	2.7	0	0.2
2K1	44081	1301	1469	140	3	19	6.1	0.2	1.3
2K2	83011	538	652	3	0	4	2.3	0	0.6
2K3	46269	412	453	3	0	2	2.3	0	0.4
3A2	63664	702	813	5	0	8	3.3	0	1
3A3	57711	258	309	3	0	1	1.7	0	0.3
3E2	48213	356	409	2	0	4	2	0	1
3E3	57162	237	268	3	0	3	1.7	0	1.1
3K2	26817	542	570	8	0	3	3.8	0	0.5
3K3	63876	327	381	3	0	3	1.8	0	0.8
4A2	80676	347	440	2	0	1	1.6	0	0.2
4A3	61320	191	226	3	0	0	1.5	0	0
4A4	69614	1080	1224	10	1	10	4.6	0.1	0.8
4E2	145729	405	560	3	2	8	1.9	0.3	1.3
4E3	53079	224	262	3	0	1	1.7	0	0.4
4E4	68318	1266	1435	28	1	26	5.4	0.1	1.7

4K2	25595	562	587	7	0	4	3.8	0	0.7
4K3	66934	460	542	3	0	4	2.3	0	0.7
4K4	53867	1308	1445	67	2	26	6	0.1	1.7
5A2	49259	440	494	6	0	3	3.2	0	0.6
5A3	53923	178	214	2	0	0	1.4	0	0
5A4	93272	1443	1690	29	2	35	5.6	0.1	2
5E2	82674	497	621	3	1	9	2.6	0.2	1.4
5E3	70366	296	346	2	0	7	1.8	0	1.9
5E4	68855	1408	1590	92	5	15	6.1	0.3	0.9
5K2	91040	680	838	6	1	14	3.2	0.1	1.6
5K3	54366	627	705	6	0	5	3.4	0	0.7
5K4	73476	1679	1913	221	1	35	6.6	0	1.7
6A3	42452	249	282	3	0	1	1.8	0	0.4
6A4	46736	763	835	4	1	13	3.7	0.1	1.5
6E3	63322	541	628	3	1	6	2.8	0.2	0.9
6E4	71477	501	597	2	1	3	2.3	0.2	0.5
6K3	27235	325	340	4	0	2	2.6	0	0.6
6K4	123486	1801	2195	65	2	45	6.2	0.1	1.9
7A1	46214	832	937	57	1	16	5.2	0.1	1.7
7A2	93221	926	1121	16	0	17	4.5	0	1.4
7A3	97430	399	515	2	0	7	1.6	0	1.3
7A4	67784	556	643	2	0	6	2.1	0	0.9
7E1	78709	1108	1284	82	0	20	5.6	0	1.5
7E2	79334	576	670	7	0	11	3.5	0	1.5
7E3	11406	108	108	3	0	1	2	0	0.9
7E4	61491	794	899	6	1	17	3.8	0.1	1.8
7K1	68100	1399	1564	224	2	21	6.3	0.1	1.3
7K2	30559	578	607	11	1	8	4.1	0.2	1.3
7K3	23119	279	285	4	0	0	2.9	0	0
8A1	167167	1231	1663	44	3	14	5.2	0.2	0.7
8A2	89281	472	579	2	0	8	2	0	1.3
8A3	95105	1151	1399	8	2	17	4.3	0.1	1.1
8A4	85462	1087	1286	7	2	22	4.2	0.1	1.6
8E1	65838	1518	1709	294	3	23	6.5	0.2	1.3
8E2	76104	599	697	6	2	12	3.5	0.3	1.6

8E3	139563	797	1040	16	1	21	4.1	0.1	1.8
8E4	89647	1380	1627	37	1	27	5.5	0.1	1.6
8K1	92541	1439	1689	157	5	22	6.3	0.3	1.2
8K2	325158	1862	2657	101	6	65	6.1	0.2	1.9
8K3	573869	1963	3078	39	16	74	5.6	0.4	1.7
8K4	210825	1273	1784	8	3	39	4	0.1	1.8

232

Table S2: Genome statistics. Summary information for genomes binned determined by CheckM.

Genome name	Genome size (MB)	GC (%)	Nr. of contigs	Completeness (%)	Contamination (%)	Heterogeneity (%)
Bin 6	2.46	56.2	235	97.84	0	0
Bin 10	2.38	51.1	112	93.1	0	0

Table S3: Average nucleotide identity (ANI) comparisons to the closest relatives using OrthoANIu algorithm [14].

Name	Contigs	Total length (bp)	GC content (%)	ANI (%)
Bin 6	235	2,460,404	56.35	85.13
Chlorobaculum parvum NCIB 8327	1	2,289,249	55.8	
Bin 10	112	2,375,588	51.44	85.82
Prosthecochloris sp. CIB 2401	1	2,399,849	52.13	

Table S4: CRISPR-Cas system information for each metagenome-assembled genome

Name	CRISPR array	contig	location (bp)	length	# spacers	DR length
Bin 6	CRISPR1	26	20933-26430	42829	82	30
Bin 6	CRISPR2	145	613-1685	16001	14	35
Bin 6	CRISPR3	145	198-278	16001	2	35
Bin 10	CRISPR1	20	3561-4695	55534	14	37
Bin 10	CRISPR2	316	7079-7510	10315	6	32
Bin 10	CRISPR3	316	10128-10293	10315	2	33

Supplementary References

1. Gower JC. Generalized Procrustes analysis. Psychometrika. 1975;40:33–51.
2. Gobet A, Böer SI, Huse SM, van Beusekom JEE, Quince C, Sogin ML, et al. Diversity and dynamics of rare and of resident bacterial populations in coastal sands. ISME J [Internet]. 2012;6:542–53. Available from: http://www.nature.com/doifinder/10.1038/ismej.2011.132
3. Eren AM, Esen C, Quince C, Vineis JH, Morrison HG, Sogin ML, et al. Anvi ' o : an advanced analysis and visualization platform for ' omics data. 2015;1–29.
4. Wattam AR, Abraham D, Dalay O, Disz TL, Driscoll T, Gabbard JL, et al. PATRIC, the bacterial bioinformatics database and analysis resource. Nucleic Acids Res [Internet]. Oxford University Press; 2014 [cited 2019 Feb 14];42:D581-91. Available from: http://www.ncbi.nlm.nih.gov/pubmed/24225323
5. Wattam AR, Davis JJ, Assaf R, Boisvert S, Brettin T, Bun C, et al. Improvements to PATRIC, the all-bacterial bioinformatics database and analysis resource center. Nucleic Acids Res. 2017;45:D535–42.
6. Makarova KS, Wolf YI, Alkhnbashi OS, Costa F, Shah SA, Saunders SJ, et al. An updated evolutionary classification of CRISPR–Cas systems. Nat Rev Microbiol [Internet]. Nature Publishing Group; 2015 [cited 2019 Feb 14];13:722–36. Available from: http://www.nature.com/articles/nrmicro3569